Electrochimica Acta 56 (2011) 10016–10022

Contents lists available at SciVerse ScienceDirect

Electrochimica Acta

journal homepage: www.elsevier.com/locate/electacta

A kinetic study of electrochemical lithium insertion in nanosized rutile β-MnO_2 by impedance spectroscopy

S. Bach[a,b,*], J.P. Pereira-Ramos[a], P. Willmann[c]

[a] *Institut de Chimie et des Matériaux Paris Est, GESMAT, UMR 7182 CNRS-Université Paris XII, 2 rue Henri Dunant 94320 Thiais, France*
[b] *Université d'Evry Val d'Essonne, Bd F.Mitterrand, Departement Chimie, 91025 Evry Cédex, France*
[c] *Centre National d'Etudes Spatiales, 118 avenue Edouard Belin, 31401 Toulouse Cedex 9, France*

ARTICLE INFO

Article history:
Received 1 July 2011
Received in revised form 24 August 2011
Accepted 25 August 2011
Available online 9 September 2011

Keywords:
Lithium batteries
Rutile β-MnO_2
Nanomaterial
Li transport
Electrochemical impedance

ABSTRACT

The kinetics of the electrochemical lithium insertion reaction in nano-sized rutile β-MnO_2 has been investigated using ac impedance spectroscopy. The experimental kinetic data are obtained for a rutile compound synthesized by ball-milling the powder produced from the heat treatment of manganese nitrate salts. The results are discussed as a function of the Li content for $0 < x < 0.6$ and the number of cycles in the 4.1–2 V window. From a comparison with data obtained on the micro-sized oxide, an improved kinetics is found with D_{Li} values for the apparent chemical diffusion coefficient of lithium much higher by one order of magnitude than in microsized oxide. Impedance behaviour of the ball-milled rutile β-MnO_2 *vs* cycles demonstrates a new system takes place from the second cycle, characterized by a significant improvement of Li diffusion by a factor 5 and a cathode impedance which decreases by a factor 2, remaining thereafter unchanged during cycling.

1. Introduction

In the field of cathode materials for secondary lithium batteries, manganese oxides have unique and important advantages over other transition metal oxides due to their low toxicity, good capacity and inexpensive cost. Manganese oxides exist in various polymorphic forms and are made of MnO_6 octahedra, these basic units being linked by sharing edges and corners to give rise to different types such as α-, β-, γ-, and λ-types. For instance the hollandite form exhibits (2 × 2) while β-MnO_2 also called pyrolusite exhibits a rutile structure which contains the narrowest (1 × 1) channels. γ-MnO_2 contains domains of intergrown β-MnO_2 and ramsdellite MnO_2 with larger channels (2 × 1) and λ-MnO_2 is characterized by a three dimensional network of channels. The lowest size of the channels available for Li transport in the β-MnO_2 oxide framework makes this electrode material cannot provide much capacity. Indeed it has been found that the Li uptake inserted chemically or electrochemically into crystallized β-MnO_2 does not exceed 0.3 Li per mole of oxide at room temperature [1,2], and nearly 1 Li at temperatures around 100 °C and 150 °C [3,4].

Very recently, nanostructured materials have stimulated numerous works reporting the positive effect of the nanosized oxide particles mainly because of their substantial advantages in terms of mass transport [5–10]. Several groups have reported that at room temperature nanometer-sized [11–14] and mesoporous [15,16] β-MnO_2 show a higher electroactivity towards Li insertion than the conventional bulk oxide with a maximum Li uptake in the range 0.66–0.92 per MnO_2 unit in the first discharge. β-MnO_2 nanomaterials with different morphologies have been synthesized via a hydrothermal route using $Mn(NO_3)_2$ solutions [11], mixtures of $KMnO_4$ and $MnCl_2$ [12] or by hydrothermal persulfate treatments of solid precursors like MnO and Mn_2O_3 [13] or by simple heating a mixture of $Mn(NO_3)_2$ and acetylene black [14]. However, in spite of the afforded improvements, the electrochemical data available on nanosized and mesoporous β-MnO_2 only consist in the discharge–charge profile for one or several cycles and cycling data obtained in various voltage windows such as 4.5–1.5 V, 5–1 V, 4–1.5 V, 4.5–1 V. Even when the stark difference for the behaviour of bulk and nanosized β-MnO_2 is reported as being caused by kinetics, no work has focused on the kinetic of the electrochemical Li insertion reaction in nanosized β-MnO_2 [11–16]. Li diffusion process in the active material is essential for a good understanding of the cathode performance. This lack of kinetic data on nanosized rutile MnO_2 prompted us to investigate using ac impedance spectroscopy the kinetics of the Li insertion process into nanosized rutile MnO_2 prepared for the first time by ball-milling. The results reported here

---

[*] Corresponding author at: Institut de Chimie et des Matériaux Paris Est, GESMAT, UMR 7182 CNRS-Université Paris XII, 2 rue Henri Dunant 94320 Thiais, France.
E-mail address: bach@glvt-cnrs.fr (S. Bach).

0013-4686/$ – see front matter © 2011 Elsevier Ltd. All rights reserved.
doi:10.1016/j.electacta.2011.08.118

are discussed as a function of the lithium content x in nanosized Li_xMnO_2 ($0 < x \leq 0.60$) and cycles.

2. Experimental

2.1. Powder preparation

The procedure used to obtain nanometric pyrolusite β-MnO_2 includes two steps. β-MnO_2 was first prepared by thermal decomposition of $Mn(NO_3)_2 \cdot 6H_2O$ at 300 °C during 5 h. The latter is named microsized material in the text. During this decomposition, oxidation occurs leading to the formation of β-MnO_2 [11,14,17]. In a second step the latter was ground in a planetary ball mill at 500 rpm for 1 h, using tungsten balls and an agate jar.

2.2. Structural characterization

XRD diffraction experiments were performed with a Inel Cps 300 diffractometer using the Cu Kα radiation ($\lambda = 1.54056$ Å). The morphology of the sample has been examined with a Philips XL 30 scanning electron microscope.

2.3. Electrochemical measurements

The electrolyte used was 1 mol L^{-1} $LiPF_6$ in ethylene carbonate (EC) and DiEthyl carbonate (DEC) solution (1:2, v/v). The working electrode consisted of a stainless steel grid (12 mm diam., 0.2 mm thickness) with a geometric area of 1 cm^2 on which the cathode material was pressed (5 t/cm^2). The cathode was made of a mixture of active material (80 wt%), acetylene black (7.5 wt%), graphite (7.5 wt%) and teflon as binder agent (5%). The film is obtained by mixing the oxide powder, carbon and teflon. Electrochemical studies were carried out in two-electrode cells (Swagelok® type) for the galvanostatic measurements and cycling tests. In that case a lithium foil was used both as reference and auxiliary electrode. Galvanostatic experiments were made with a MacPile apparatus. For GITT measurements, each electrode was discharged by the application of cathodic current (100 μA) for 1 h. After this interval, the discharge current was switched off and the potential of the electrode allowed to equilibrate up to voltage remained less than 0.2 mV for 1 h.

Impedance measurements were performed using a three-electrode cell in the frequency range 4×10^4–7×10^{-3} Hz with an E.G.G. 273A apparatus connected with a Solartron SI 1255 frequency analyser driven by an IBM computer. The reference and counter electrodes consisted respectively of a lithium wire in a separated compartment and a high surface gold wire. The excitation signal was 10 mV peak to peak. The equilibrium potential was considered to be reached when the drift in open circuit voltage remained less than 0.2 mV for 1 h.

3. Results and discussion

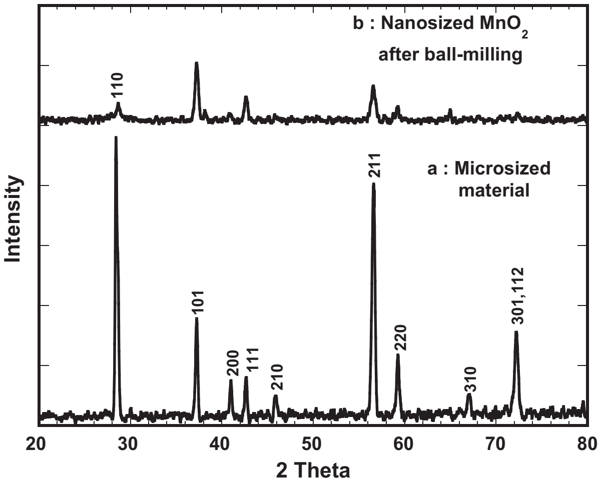

Fig. 1. Comparison of the X-ray diffraction patterns (Cu Kα) of (a) the microsized material and (b) the nano-sized β-MnO_2.

Fig. 1 shows the XRD diffraction patterns of the prepared powder compared with that of the starting compound (Fig. 1). The whole pattern can be indexed on the basis of a β-MnO_2 rutile single phase (space group $P4_2/mnm$). The lattice parameters calculated from XRD data are $a = 4.381$ Å and $c = 2.877$ Å in good agreement with those of the starting material ($a = 4.398$ Å and $c = 2.873$ Å, JCPDS 71-0071). In the β-MnO_2 rutile structure, each metal atom is surrounded by six oxygen atoms and octahedral share edges to form single chains of octahedral extending along the c axis, giving a (1 × 1)-tunnel structure (Fig. 2). The broader peaks found for all the diffraction lines of the nanosized powder prepared by ball-milling technique suggest a smaller grain size, corresponding to a nanosized material. The mean crystallite size calculated from the XRD pattern using Scherrer's equation for (1 1 0) and (1 0 1) plane is 40 nm and 35 nm, respectively against few micrometers for the starting material.

From SEM images (Fig. 3c and d), it can be seen the starting powder consists of large aggregates of ≈10 μm made of agglomerated taping micrometric grains with a rough surface. Compared to Fig. 3c, the ball-milled sample exhibits smaller particles with an homogeneous particle size distribution, in the range 100–200 nm (Fig. 3a and b). The particles seem to be interlocked and large voids appear which can promote an excellent soaking of the oxide material in the electrolyte allowing then a high surface area to be available for electrochemical experiments.

A comparison of the first discharge–charge profiles for the microsized and the nanosized rutile β-MnO_2 is reported in Fig. 4. The first discharge curves of nanosized β-MnO_2 at C/20 (Fig. 4b) show a flat discharge plateau between 2.9 and 2.7 V. At room temperature, the comparison of the electrochemical

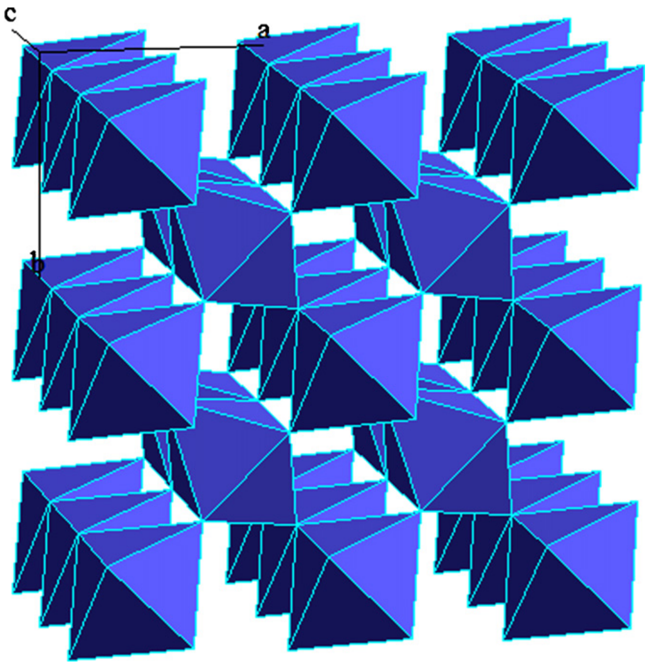

Fig. 2. Crystal structure along the 0 0 1 direction of rutile β-MnO_2. Mn is located in octahedral sites.